

Synthesis and Characterization of the Benzoylformate Ferrous Complexes with the Hindered Tris(pyrazolyl)borate Ligand as a Structural Model for Mononuclear Non-Heme Iron Enzymes[†]

Shiro Hikichi,* Tamako Ogihara, Kiyoshi Fujisawa, Nobumasa Kitajima, Munetaka Akita, and Yoshihiko Moro-oka*

Research Laboratory of Resources Utilization, Tokyo Institute of Technology, 4259 Nagatsuta, Midori-ku, Yokohama 226, Japan

Received August 1, 1996[⊗]

By using a hindered tripodal ligand, hydrotris(3-*tert*-butyl-5-isopropylpyrazol-1-yl)borate HB(3-*t*Bu-5-*i*Prpz)₃, a series of monomeric ferrous complexes having acetate, hydroxide, and benzoylformate ligands were synthesized. Reaction of KHB(3-*t*Bu-5-*i*Prpz)₃ with anhydrous Fe(OAc)₂ yielded acetato complexes Fe(OAc)[HB(3-*t*Bu-5-*i*Prpz)₃] (1) and Fe(OAc)[HB(3-*t*Bu-5-*i*Prpz)₃](3-*i*Pr-5-*t*BupzH) (2). A hydroxo complex Fe(OH)[HB(3-*t*Bu-5-*i*Prpz)₃] (3) was prepared by the treatment of 1 or 2 with aqueous NaOH. The geometry of Fe(II) in 3 is a slightly distorted tetrahedron as determined by X-ray crystallography. The hydroxo complex 3 reacted with benzoylformic acid to give the benzoylformate complex Fe(O₂CC(O)Ph)[HB(3-*t*Bu-5-*i*Prpz)₃] (4), which showed thermochromism which depended on the coordination geometry of the benzoylformate ligand. The Fe(II) ion in the colorless form of 4 isolated at 4 °C is coordinated by a tetrahedral N₃O₁ ligand donor set including the unidentate benzoylformate ligand. On the other hand, the bluish purple form of 4 isolated at -20 °C has a five-coordinate trigonal bipyramidal Fe(II) center. The benzoylformate ligand in this bluish purple form works as a chelate ligand through coordination of the unidentate carboxylate oxygen atom as well as the ketonic oxygen atom. A benzoylformate complex containing an additional pyrazole, Fe(O₂CC(O)Ph)[HB(3-*t*Bu-5-*i*Prpz)₃](3-*i*Pr-5-*t*BupzH) (5), was obtained by the reaction of 3 with benzoylformic acid in the presence of 3-*tert*-butyl-5-isopropylpyrazole. The iron atom in 5 is coordinated by an N₄O₁ ligand donor set with trigonal bipyramidal geometry. A hydrogen-bonding interaction between the carboxylate oxygen atom and the additional pyrazole's NH proton in 5 is suggested from the short distance between O_{carboxylate} and N_{pyrazole} observed in the X-ray structure and the absence of the νNH vibration in the IR spectrum.

Introduction

In biological systems, many heme and non-heme iron proteins take part in dioxygen metabolism.¹ For many years, a class of non-heme iron proteins containing a dinuclear site (e.g., hydroxylase of methane monooxygenase,² ribonucleotide reductase,³ and hemerythrin⁴) have attracted much attention because of their unique physicochemical properties and reactivities attributed to the diiron core. Recent X-ray crystal-

lographic and spectroscopic studies of these enzymes have led to the elucidation of the structure of the diiron reaction center, while their mechanisms of dioxygen activation remain to be elucidated. A diferric μ-peroxo intermediate has been characterized recently in the reaction cycle of MMO hydroxylase.⁵ A variety of mononuclear non-heme iron enzymes which catalyze oxygenation or oxidation are also known.⁶ Although studies about “mononuclear” enzymes have lagged behind those of the “dinuclear” enzymes, interest in the dioxygen activation mononuclear non-heme iron enzymes is rapidly growing.^{1f} The

[†] Abbreviations used are as follows: HB(3,5-*i*Prpz)₃, hydrotris(3,5-diisopropylpyrazol-1-yl)borate (monoanion); HB(3-*t*Bu-5-*i*Prpz)₃, hydrotris(3-*tert*-butyl-5-isopropylpyrazol-1-yl)borate (monoanion); 3-*t*Bu-5-*i*PrpzH, 3-*tert*-butyl-5-isopropylpyrazole; 3-*i*Pr-5-*t*BupzH, 3-isopropyl-5-*tert*-butylpyrazole; 3,5-*i*PrpzH, 3,5-diisopropylpyrazole; OAc, acetate; BF, benzoylformate.

[⊗] Abstract published in *Advance ACS Abstracts*, August 15, 1997.

- (1) (a) Springer, B. A.; Sliagar, S. G.; Olson, J. S.; Phillips, G. N., Jr. *Chem. Rev.* **1994**, *94*, 699. (b) Momenteau, M.; Reed, C. A. *Chem. Rev.* **1994**, *94*, 659. (c) Feig, A. L.; Lippard, S. J. *Chem. Rev.* **1994**, *94*, 759. (d) Sanders-Loehr, J. In *Iron Carriers and Iron Proteins*; Loehr, T. M., Ed.; VCH: New York, 1989; Vol. 5, p 373. (e) Vincent, J. B.; Olivier-Lilley, G. L.; Averill, B. A. *Chem. Rev.* **1990**, *90*, 1447. (f) Nivorozhkin, A. L.; Girerd, J.-J. *Angew. Chem. Int. Ed. Engl.* **1996**, *35*, 609.
- (2) (a) Liu, K. E.; Feig, A. L.; Goldberg, D. P.; Watton, S. P.; Lippard, S. J. In *Applications of Enzyme Biotechnology*; Kelly, J. W., Ed.; Plenum: New York, 1993; p 301. (b) Fox, B. G.; Lipscomb, J. D. In *Biological Oxidation Systems*; Reddy, C. C., Ed.; Academic: New York, 1990; Vol. 1, p 367. (c) Rosenzweig, A. C.; Frederick, C. A.; Lippard, S. J.; Nordlund, P. *Nature* **1993**, *366*, 537.
- (3) (a) Fontecave, M.; Nordlund, P.; Eklund, H.; Reichard, P. In *Advances in Enzymology and Related Areas of Molecular Biology*; Meister, A., Ed.; Wiley and Sons: New York, 1992; Vol. 65, p 147. (b) Nordlund, P.; Sjöberg, B.-M.; Eklund, H. *Nature* **1990**, *345*, 593. (c) Nordlund, P.; Eklund, H. *J. Mol. Biol.* **1993**, *232*, 123.

- (4) (a) Stenkamp, R. E. *Chem. Rev.* **1994**, *94*, 715. (b) Stenkamp, R. E.; Sieker, L. C.; Jensen, L. H. *J. Am. Chem. Soc.* **1984**, *106*, 618. (c) Sheriff, S.; Hendrickson, W. A.; Smith, J. L. *J. Mol. Biol.* **1987**, *197*, 273. (d) Holms, M. A.; Stenkamp, R. E. *J. Mol. Biol.* **1991**, *220*, 723.
- (5) Liu, K. E.; Valentine, A. M.; Qiu, D.; Edmondson, D. E.; Appleman, E. H.; Spiro, T. G.; Lippard, S. J. *J. Am. Chem. Soc.* **1995**, *117*, 4997.
- (6) (a) Fridovich, I. *Acc. Chem. Res.* **1982**, *15*, 200. (b) Dix, T. A.; Bollag, G. E.; Domanico, P. L.; Benkovic, S. J. *Biochemistry* **1985**, *24*, 2955. (c) Dix, T. A.; Benkovic, S. J. *Biochemistry* **1985**, *24*, 5839. (d) Benkovic, S. J.; Bloom, L. M.; Bollag, G.; Dix, T. A.; Gaffney, B. J.; Pember, S. *Ann. N.Y. Acad. Sci.* **1986**, *471*, 226. (e) Dix, T. A.; Kuhn, D. M.; Benkovic, S. J. *Biochemistry* **1987**, *26*, 3354. (f) Andersson, K. K.; Cox, D. D.; Que, L., Jr.; Flatmark, T.; Haavik, J. *J. Biol. Chem.* **1988**, *263*, 18621. (g) Ruettinger, R. T.; Griffith, G. R.; Coon, M. J. *Arch. Biochem. Biophys.* **1977**, *183*, 528. (h) Katopodis, A. G.; Wimalasena, K.; Lee, J.; May, S. W. *J. Am. Chem. Soc.* **1984**, *106*, 7298. (i) Que, L., Jr. In *Iron Carriers and Iron Proteins*; Loehr, T. M., Ed.; VCH: New York, 1989; Vol. 5, p 467. (j) Crutcher, S. E.; Geary, P. J. *Biochem. J.* **1979**, *177*, 393. (k) Geary, P. J.; Dickson, D. P. E. *Biochem. J.* **1981**, *195*, 199. (l) Veldink, G. A.; Vliegthart, J. F. G. *Adv. Inorg. Biochem.* **1984**, *6*, 139. (m) Nelson, M. J.; Cowling, R. A. *J. Am. Chem. Soc.* **1990**, *112*, 2820. (n) Hanauke-Abel, H. M.; Gunzler, V. *J. Theor. Biol.* **1982**, *94*, 421. (o) Kivirikko, K. I.; Myllyla, R.; Pihlajaniemi, T. *FASEB J.* **1989**, *3*, 1609.

structures of iron SOD,⁷ protocatechuate 3,4-dioxygenase,⁸ lipoyxygenase,⁹ 2,3-dihydroxybiphenyl 1,2-dioxygenase,¹⁰ and isopenicillin N synthase (Mn substituted form)¹¹ were recently solved by X-ray crystallography, providing some structural information associated with the iron metal center. However, the coordination modes of dioxygen in these enzymes are not established.

Many synthetic Fe(III) compounds have provided various chemical insights into the trivalent state of mono- and dinuclear iron sites.¹² On the other hand, Fe(II) complexes modeling the divalent state of iron sites have been studied less extensively than Fe(III) model complexes. We have previously succeeded in the preparation of the monomeric carboxylato Fe(II) complexes¹³ and the dinuclear di- μ -hydroxo and μ -hydroxo- μ -carboxylato Fe(II) complexes¹⁴ by using the tripodal ligand hydrotris(3,5-diisopropylpyrazol-1-yl)borate, HB(3,5-iPr₂pz)₃. These monomeric carboxylato complexes are capable of reversible dioxygen uptake to give the dinuclear adduct bridged by a μ -peroxo ligand.^{13,15} Que *et al.*¹⁶ and Valentine *et al.*¹⁷ recently studied benzoylformato Fe(II) complexes as a model for α -keto acid-dependent non-heme iron enzymes, which catalyze oxygenation of substrates by O₂ with concomitant oxygenation and decarboxylation of the α -keto acid cofactor to produce CO₂ and succinate.^{1c,6n,o} We report here syntheses of mononuclear acetato, hydroxo, and benzoylformato Fe(II) complexes and their characterization in order to gain structural and chemical insights into the reduced state of the mononuclear iron site. In the present study, a sterically hindered hydrotris(pyrazolyl)borate ligand, HB(3-tBu-5-iPrpz)₃, was adopted to isolate the monomeric complexes.

Experimental Section

Instrumentation. ¹H-NMR spectra were recorded on a JEOL-GX-270 (270 MHz for ¹H) spectrometer. The chemical shifts are reported

- (7) (a) Ringe, D.; Petsko, G. A.; Yamakura, F.; Suzuki, K.; Ohmori, D. *Proc. Natl. Acad. Sci. U.S.A.* **1983**, *80*, 3879. (b) Stallings, W. C.; Powers, T. B.; Patridge, K. A.; Fee, J. A.; Ludwig, M. L. *Proc. Natl. Acad. Sci. U.S.A.* **1983**, *80*, 3884. (c) Stoddard, B. L.; Howell, P. L.; Ringe, D.; Petsko, G. A. *Biochemistry* **1990**, *29*, 8885. (d) Lah, M. S.; Dixon, M. M.; Patridge, K. A.; Stallings, W. C.; Fee, J. A.; Ludwig, M. L. *Biochemistry* **1995**, *34*, 1646. (e) Cooper, J. B.; McIntyre, K.; Badasso, M. O.; Wood, S. P.; Zhang, Y.; Garbe, T. R.; Young, D. J. *Mol. Biol.* **1995**, *246*, 531.
- (8) (a) Ohlendorf, D. H.; Weber, P. C.; Lipscomb, J. D. *J. Mol. Biol.* **1987**, *195*, 225. (b) Ohlendorf, D. H.; Lipscomb, J. D.; Weber, P. C. *Nature* **1988**, *336*, 403. (c) Ohlendorf, D. H.; Orville, A. M.; Lipscomb, J. D. *J. Mol. Biol.* **1994**, *244*, 586.
- (9) (a) Boyington, J. C.; Gaffney, B. J.; Amzel, L. M. *Science* **1993**, *260*, 1482. (b) Minor, W.; Steczko, J.; Bolin, J. T.; Otwinowski, Z.; Axelrod, B. *Biochemistry* **1993**, *32*, 6320.
- (10) (a) Han, S.; Eltis, L. D.; Timms, K. N.; Muchmore, S. W.; Bolin, J. T. *Science* **1995**, *270*, 976. (b) Senda, T.; Sugiyama, K.; Narita, H.; Yamamoto, T.; Kimbara, K.; Fukuda, M.; Sato, M.; Yano, K.; Mitsui, Y. *J. Mol. Biol.* **1996**, *255*, 735.
- (11) Roach, P. L.; Clifton, I. J.; Fülöp, V.; Harlos, K.; Barton, G. J.; Hajdu, J.; Andersson, I.; Schofield, C. J.; Baldwin, J. E. *Nature* **1995**, *375*, 700.
- (12) (a) Lippard S. *J. Angew. Chem., Int. Ed. Engl.* **1988**, *27*, 344. (b) Que, L., Jr.; True, A. E. *Prog. Inorg. Chem.* **1990**, *38*, 97. (c) Kurtz, D. M., Jr. *Chem. Rev.* **1990**, *90*, 585.
- (13) (a) Kitajima, N.; Fukui, H.; Moro-oka, Y.; Mizutani, Y.; Kitagawa, T. *J. Am. Chem. Soc.* **1990**, *112*, 6402. (b) Kitajima, N.; Tamura, N.; Amagai, H.; Fukui, H.; Moro-oka, Y.; Mizutani, Y.; Kitagawa, T.; Mathur, R.; Heerwegh, K.; Reed, C. A.; Randall, C. R.; Que, L., Jr.; Tatum, K. *J. Am. Chem. Soc.* **1994**, *116*, 9071.
- (14) Kitajima, N.; Tamura, N.; Tanaka, M.; Moro-oka, Y. *Inorg. Chem.* **1992**, *31*, 3342.
- (15) Very recently, a molecular structure of a dinuclear Fe(III) μ -1,2-peroxo-bis(μ -carboxylato) complex bearing the HB(3,5-iPr₂pz)₃ ligand has been reported: Kim, K.; Lippard, S. J. *J. Am. Chem. Soc.* **1996**, *118*, 4914.
- (16) (a) Chiou, Y.-M.; Que, L., Jr. *J. Am. Chem. Soc.* **1995**, *117*, 3999. (b) Chiou, Y.-M.; Que, L., Jr. *J. Am. Chem. Soc.* **1992**, *114*, 7567. (c) Chiou, Y.-M.; Que, L., Jr. *Angew. Chem., Int. Ed. Engl.* **1994**, *33*, 1886. (d) Chiou, Y.-M.; Que, L., Jr. *Inorg. Chem.* **1995**, *34*, 3270.

as values (δ , ppm) downfield from the internal standard Me₄Si. IR measurements were carried out in KBr using a JASCO FT/IR-5300 instrument. Electronic spectra were recorded on a Shimadzu UV-260 spectrometer. Low-temperature electronic spectra were obtained using an Oxford DN1704 cryostat. Field desorption mass spectra were recorded on a Hitachi M-80 mass spectrometer. The X-ray data collections were performed on Rigaku four-circle AFC-5S and AFC-5R diffractometers. The X-ray data analysis were completed by TEXSAN on an Indigo-IRIS computer (Silicon Graphics), obtained from Rigaku.

Materials and Methods. All solvents used were purified by literature methods.¹⁸ Reagents of the highest grade commercially available were used without further purification. All manipulations were performed under argon by standard Schlenk techniques. Details for the preparation of KHB(3-tBu-5-iPrpz)₃ will be described elsewhere.¹⁹

Fe(OAc)[HB(3-tBu-5-iPrpz)₃] (1). K[HB(3-tBu-5-iPrpz)₃] (2.51 g; 4.59 mmol) was stirred with 1 equiv of Fe(OAc)₂ (1.02 g; 5.84 mmol) in a mixture of CH₂Cl₂ (25 mL) and MeCN (5 mL) overnight. The precipitate formed was removed by filtration, and the filtrate was dried under vacuum. Extraction of the resulting white solid with 30 mL of pentane and cooling at -20 °C overnight afforded **1** as a colorless crystalline solid (1.09 g; 1.74 mmol; 38%). Anal. Calcd for C₃₂H₅₅N₆O₂BFe: C, 61.74; H, 8.91; N, 13.50. Found: C, 61.45; H, 9.09; N, 13.32. IR (KBr, cm⁻¹): 2564 (BH), 1572 (COOas). ¹H-NMR (C₆D₆, 27 °C): δ -6.9 (br, 27H, *tBu*), 7.0 (18H, CHMe₂), 22.7 (3H, CHMe₂), 28.3 (1H, BH), 59.9 (3H, *pz-4H*), 118.7 (3H, OAc). FD-MS (*m/z*): 622.

Fe(OAc)[HB(3-tBu-5-iPrpz)₃](3-iPr-5-tBupzH) (2). Cooling the filtrate of **1** (see above) at -20 °C afforded **2** as colorless crystals (0.85 g; 1.07 mmol; 23%). Anal. Calcd for C₄₂H₇₃N₈O₂BFe: C, 63.96; H, 9.33; N, 14.21. Found: C, 64.43; H, 9.46; N, 14.09. IR (KBr, cm⁻¹): 2567 (BH), 1583 (COOas). ¹H-NMR (C₆D₆, 27 °C): δ -2.4 (br, 27H, *tBu*), 5.6 (18H, CHMe₂), 17.7 (3H, CHMe₂), 57.7 (3H, *pz-4H*), 94.7 (3H, OAc). FD-MS (*m/z*): 622.

Fe(OH)[HB(3-tBu-5-iPrpz)₃] (3). A toluene solution (15 mL) of **1** (0.47 g; 0.60 mmol) was treated with 7.5 mL of 1 N aqueous NaOH for 30 min under argon. The toluene phase was separated and dried under vacuum. The resulting white solid was recrystallized from a mixture of MeCN and CH₂Cl₂ at -20 °C, and **3** was obtained as colorless crystals (0.17 g; 0.29 mmol; 48%). Anal. Calcd for C₃₀H₅₃N₆OBF_e: C, 62.08; H, 9.20; N, 14.48. Found: C, 61.79; H, 8.88; N, 14.27. IR (KBr, cm⁻¹): 3695 (OH), 2547 (BH). ¹H-NMR (C₆D₆, 27 °C): δ -28.9 (br, 27H, *tBu*), 16.4 (18H, CHMe₂), 47.8 (3H, CHMe₂), 56.7 (3H, *pz-4H*). FD-MS (*m/z*): 580.

Fe(O₂CC(O)Ph)[HB(3-tBu-5-iPrpz)₃] (4). A CH₂Cl₂ solution (15 mL) of **3** (0.27 g; 0.46 mmol) was stirred with 1 equiv of benzoylformic acid for 30 min. After removal of the solvent under vacuum, the resulting pale purple solid was dissolved in MeCN. Crystallization at 4 °C afforded **4** as colorless crystals (0.25 g; 0.33 mmol; 73%). Anal. Calcd for C₃₈H₅₇N₆O₃BFe: C, 64.05; H, 8.06; N, 11.79. Found: C, 63.78; H, 8.18; N, 12.16. IR (KBr, cm⁻¹): 2569 (BH), 1694 (C=O), 1666 (COOas), 1598 (PhC=C). ¹H-NMR (toluene-*d*₈, 27 °C): δ -8.5 (br, 27H, *tBu*), 8.9 (18H, CHMe₂), 11.3 (1H, *p-Ph*), 12.2 (2H, *m-Ph*), 25.2 (2H, *o-Ph*), 29.5 (3H, CHMe₂), 41.2 (br, 1H, BH), 63.0 (3H, *pz-4H*); (-60 °C) -17.6 (br, 27H, *tBu*), 13.5 (18H, CHMe₂), 14.8 (2H, *m-Ph*), 16.0 (1H, *p-Ph*), 37.8 (2H, *o-Ph*), 42.4 (3H, CHMe₂), 65.1 (br, 1H, BH), 86.0 (3H, *pz-4H*). FD-MS (*m/z*): 753. UV-vis (in CH₂Cl₂ solution, nm, ϵ , M⁻¹ cm⁻¹): 22 °C, 558.4 (30); -20 °C, 564.8 (148), 621.2 (130). The bluish purple form of **4** was obtained as follows: a pentane solution of the colorless solid stood at -78 °C for 1 day. Then, the solution was concentrated under vacuum and cooled at -20 °C overnight, affording 4-C₃H₁₂ as bluish purple plates.

Fe(O₂CC(O)Ph)[HB(3-tBu-5-iPrpz)₃](3-iPr-5-tBupzH) (5). To a mixture of **3** (0.12 g; 0.21 mmol) and 1 equiv of 3-*tert*-butyl-5-isopropylpyrazole (35.7 mg; 0.21 mmol) dissolved in 15 mL of CH₂-Cl₂ was added 1 equiv of benzoylformic acid (32.2 mg; 0.21 mmol),

- (17) Ha, E. H.; Ho, R. Y. N.; Kisiel, J. F.; Valentine, J. S. *Inorg. Chem.* **1995**, *34*, 2265.
- (18) Perrin, D. D.; Armarego, W. L.; Perrin, D. R. *Purification of Laboratory Chemicals*, 2nd ed.; Pergamon: New York, 1980.
- (19) Fujisawa, K.; Kitajima, N.; Moro-oka, Y. Manuscript in preparation.

Table 1. Crystal Data and Data Collection Details of **3**, **4**·MeCN (Colorless), **4**·C₅H₁₂ (Bluish Purple), and **5**

complex	3	4 ·MeCN (colorless)	4 ·C ₅ H ₁₂ (bluish purple)	5
formula	C ₃₀ H ₅₃ N ₆ OBF _e	C ₄₀ H ₆₀ N ₇ O ₃ BF _e	C ₄₃ H ₆₉ N ₆ O ₃ BF _e	C ₄₈ H ₇₅ N ₈ O ₃ BF _e
formula weight	580.45	753.62	784.71	878.83
cryst syst	orthorhombic	orthorhombic	monoclinic	orthorhombic
space group	<i>Cmc</i> 2 ₁	<i>P</i> 2 ₁ 2 ₁ 2	<i>P</i> 2 ₁ / <i>a</i>	<i>Pbca</i>
<i>a</i> /Å	16.598(3)	17.179(3)	25.387(7)	15.443(2)
<i>b</i> /Å	10.321(3)	25.369(4)	18.768(6)	17.411(2)
<i>c</i> /Å	19.908(4)	9.779(2)	9.598(2)	37.994(4)
α/deg	90	90	90	90
β/deg	90	90	97.15(2)	90
γ/deg	90	90	90	90
<i>V</i> /Å ³	3410(2)	4262(1)	4537(4)	10215(3)
<i>Z</i>	4	4	4	8
<i>D</i> (calcd)/g·cm ⁻³	1.13	1.17	1.15	1.14
cryst size/mm	0.5 × 0.3 × 0.3	0.1 × 0.01 × 0.2	0.2 × 0.03 × 0.1	0.3 × 0.3 × 0.15
data collection temp/°C	23	23	-65	23
diffractometer	Rigaku AFC-5R	Rigaku AFC-5S	Rigaku AFC-5S	Rigaku AFC-5S
radiation		graphite-monochromated Mo Kα	Mo Kα (λ = 0.710 68 Å)	
μ(Mo Kα)/cm ⁻¹	4.72	3.93	3.71	3.40
scan mode	ω	ω	ω-2θ	ω-2θ
scan width/deg	1.47 + 0.14 tan θ	1.30 + 0.14 tan θ	1.30 + 0.14 tan θ	1.30 + 0.14 tan θ
scan speed/deg·min ⁻¹	16	6	6	6
2θ range/deg	5-50	3-50	5-45	5-50
octant measd	+ <i>h</i> ,+ <i>k</i> ,+ <i>l</i>	+ <i>h</i> ,+ <i>k</i> ,+ <i>l</i>	± <i>h</i> ,+ <i>k</i> ,+ <i>l</i>	+ <i>h</i> ,+ <i>k</i> ,+ <i>l</i>
no. of measd rflns	1704	4247	6580	8797
no. of obsd rflns	1455	2805	2993	3355
	(<i>I</i> > 3σ(<i>I</i>))	(<i>I</i> > 2σ(<i>I</i>))	(<i>I</i> > 1.2σ(<i>I</i>))	(<i>I</i> > 1.5σ(<i>I</i>))
no. of params refined	222	468	488	541
data to parameters ratio	6.6	6.0	6.1	6.2
<i>p</i> -factor	0.01	0.01	0.03	0.02
<i>R</i> /%	3.46	6.65	7.91	8.69
<i>R</i> _w /%	3.88	6.22	7.67	8.27

and the mixture was stirred for 30 min. After removal of the solvent under vacuum, the resulting pale purple solid was dissolved in MeCN. Crystallization at 4 °C afforded **5** as pale yellow crystals (50.1 mg; 0.057 mmol; 27%). Anal. Calcd for C₄₈H₇₄N₈O₃BF_e: C, 65.68; H, 8.50; N, 12.77. Found: C, 65.46; H, 8.92; N, 12.65. IR (KBr, cm⁻¹): 2563 (BH), 1692 (C=O), 1604 (COOas and PhC=C). ¹H-NMR (toluene-*d*₈, 27 °C): δ -4.2 (br, 27H, *t*Bu), 7.7 (18H, CHMe₂), 10.8 (1H, *p*-Ph), 11.5 (2H, *m*-Ph), 21.7 (2H, *o*-Ph), 24.4 (3H, CHMe₂), 29.1 (br, 1H, BH), 61.4 (3H, *pz*-4H). FD-MS (*m/z*): 753.

X-ray Data Collection and Structural Determination. Single crystals of **3** were obtained by recrystallization from MeCN/CH₂Cl₂ at 4 °C. Crystals suitable for X-ray diffraction of **4**·MeCN (colorless form) and **5** were obtained from MeCN solutions at 4 °C under an argon atmosphere. Single crystals of the bluish purple form of **4** were obtained as described above. The data collections of **3**, **4**·MeCN, and **5** were completed at 23 °C with sealing crystals in a thin-wall glass capillary. The data of **4**·C₅H₁₂ (bluish purple form) were collected at -65 °C. A Mo X-ray source equipped with a graphite monochromator (Mo Kα, λ = 0.710 680 Å) was used. Automatic centering and least-squares routines were carried out for all the compounds with 25 reflections of 20° < 2θ < 25° to determine the cell parameters. Data collections were completed with ω-2θ or ω scans. A summary of the cell parameters, data collection conditions, and refinement results for **3**, **4**·MeCN, **4**·C₅H₁₂, and **5** is provided in Table 1.

The structures of the complexes were solved by the direct method (SAPI-91). Subsequent difference Fourier syntheses easily located all non-hydrogen atoms. All the non-hydrogen atoms except the disordered methyl group carbon atoms at the 5-*i*Pr substituents in **4**·MeCN and **5** and at the 5-*t*Bu substituent in **5** were refined anisotropically by TEXSAN. Those disordered methyl group carbons were refined isotropically. All the hydrogen atoms except those on the disordered

carbon atoms in **3**, **4**·MeCN, and **5** and the MeCN in **4**·MeCN were located at the calculated positions and were not refined (*d*(C-H) = 0.95 Å with the isotropic thermal factor of *U*_{iso}(H) = 1.2*U*_{iso}(C)). The final *R* and *R*_w factors are given in Table 1, where *R* = Σ(|*F*_o| - |*F*_c|)/Σ|*F*_o| and *R*_w = [Σ(w(|*F*_o| - |*F*_c|)²/Σw|*F*_o|²)]^{1/2} with *w* = 1/σ²(*F*_o) = 4*F*_o²/σ²(*F*_o²).

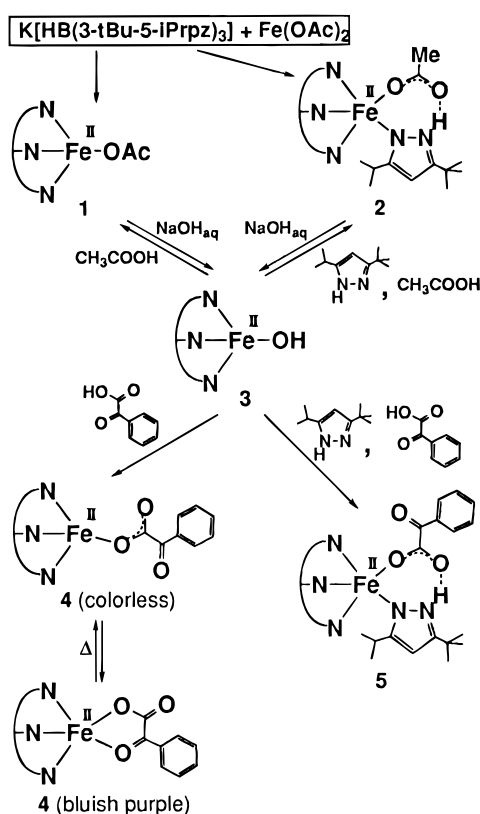
Full bond lengths, bond angles, atomic coordinates, and isotropic and anisotropic thermal parameters for **3**, **4**·MeCN, **4**·C₅H₁₂, and **5** are available as Supporting Information.

Results and Discussion

Synthesis of Monomeric Fe(II) Compounds. The benzoylformate Fe(II) complexes have been prepared successfully by dehydration condensation of the highly basic, monomeric hydroxo complex Fe(OH)[HB(3-*t*Bu-5-*i*Prpz)₃] (**3**) with the corresponding carboxylic acid as summarized in Scheme 1. In previous papers we reported the synthesis of divalent metal hydroxide complexes with the HB(3,5-*i*Prpz)₃ ligand by the hydrolysis of the corresponding carboxylate and halide complexes, which were prepared by the reaction of the appropriate metal salts with K[HB(3,5-*i*Prpz)₃].^{14,20} However, the reaction of the more bulky HB(3-*t*Bu-5-*i*Prpz)₃ ligand turned out to be a little bit different from that of the HB(3,5-*i*Prpz)₃ ligand. Reaction of anhydrous Fe(OAc)₂ with the potassium salt K[HB(3-*t*Bu-5-*i*Prpz)₃] afforded two acetate complexes: not only the desired complex (**1**) but also one containing an additional pyrazole ligand (**2**). The additional pyrazole might come from partial decomposition of the hydrotris(pyrazolyl)borate ligand. Subsequent treatment of **1** or **2** with aqueous NaOH solution resulted in the hydrolysis of the acetate part and the formation of **3**. As expected, the resulting monomeric hydroxo complex **3** was basic enough to react with carboxylic acids such as acetic acid and benzoylformic acid to give the corresponding pyrazole-free carboxylate Fe(II) complexes **1** and **4**, respectively. The condensation of **3** in the presence of external pyrazole produced the Fe(II) complexes with the carboxylate-pyrazole chelate ring

(20) (a) Kitajima, N.; Singh, U. P.; Amagai, H.; Osawa, M.; Moro-oka, Y. *J. Am. Chem. Soc.* **1991**, *113*, 7757. (b) Ito, M.; Amagai, H.; Fukui, H.; Kitajima, N.; Moro-oka, Y. *Bull. Chem. Soc. Jpn.* **1996**, *69*, 1937. (c) Kitajima, N.; Hikichi, S.; Tanaka, M.; Moro-oka, Y. *J. Am. Chem. Soc.* **1993**, *115*, 5496. (d) Kitajima, N.; Fujisawa, K.; Moro-oka, Y. *Inorg. Chem.* **1990**, *29*, 357. (e) Kitajima, N.; Fujisawa, K.; Moro-oka, Y. *J. Am. Chem. Soc.* **1990**, *112*, 3210. (f) Kitajima, N.; Fujisawa, K.; Fujimoto, C.; Moro-oka, Y.; Hashimoto, S.; Kitagawa, T.; Toriumi, K.; Tatsumi, K.; Nakamura, A. *J. Am. Chem. Soc.* **1992**, *114*, 1277.

Scheme 1



(2 and 5). The characterization of the Fe(II) complexes thus obtained is described below in detail.

(a) Acetato Complexes 1 and 2. The IR spectra of **1** and **2** clearly revealed the difference in the coordination environments of the acetate ligands. The asymmetric vibration of the COO linkage of **2** (1583 cm^{-1}) appeared at higher energy than that of **1** (1572 cm^{-1}), but the value was comparable to that of manganese(II) complex $\text{Mn}(\text{OAc})[\text{HB}(\text{3-tBu-5-iPrpz})_3](\text{3-iPr-5-tBupzH})$ (1589 cm^{-1}).²¹ The absence of a pyrazole νNH band in the spectra of **2** and the Mn complex in the range $3400\text{--}3100\text{ cm}^{-1}$ is attributed to a hydrogen-bonding interaction between the additional pyrazole's NH and the acetate oxygen atoms, which is supported by the $\text{AcO}\cdots\text{N}(\text{pyrazole})$ distance (2.65 \AA) of the Mn complex. A similar hydrogen-bonding interaction was previously observed for $\text{Mn}(\text{O}_2\text{CPh})[\text{HB}(\text{3,5-iPr}_2\text{pz})_3](\text{3,5-iPr}_2\text{pzH})$, which also lacked a pyrazole νNH vibration.²²

The $^1\text{H-NMR}$ spectra of **1** and **2** recorded at $27\text{ }^\circ\text{C}$ are reproduced in Figure 1. The assignment of the signals of **1** is based on the intensities and a comparison with the assignment of $\text{Fe}(\text{OAc})[\text{HB}(\text{3,5-iPr}_2\text{pz})_3]$ previously reported.^{13b} The spectra of **1** and **2** show similar but slightly different features; broad signals corresponding to the pyrazole's protons are observed around $0\text{--}10\text{ ppm}$ in the spectrum of **2**. The FD-MS spectra of **1** and **2** contained a peak of the same mass number ($m/z = 622$) corresponding to the pyrazole-free acetato complex. Thus, the additional pyrazole ligand of **2** probably dissociates in

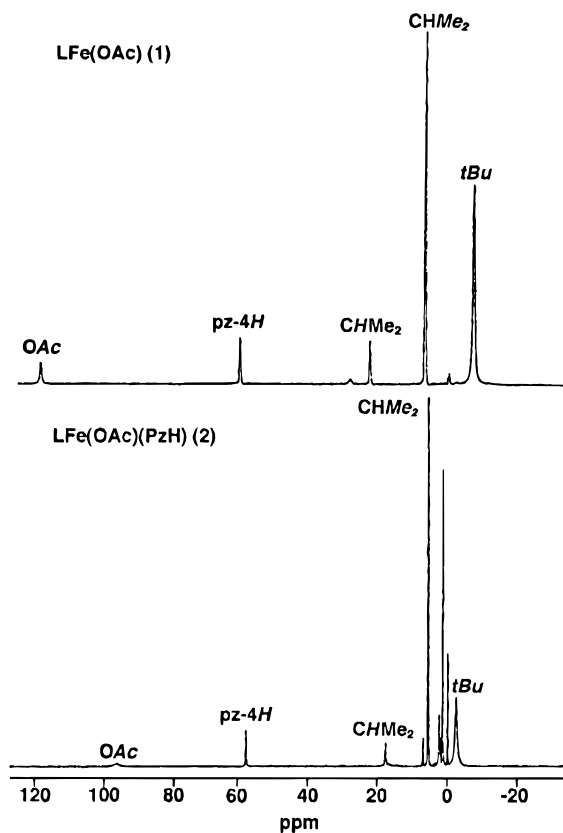


Figure 1. $^1\text{H-NMR}$ spectra of Fe(II) acetato complexes recorded in C_6D_6 solution at $27\text{ }^\circ\text{C}$. Top: $\text{Fe}(\text{OAc})[\text{HB}(\text{3-tBu-5-iPrpz})_3]$ (**1**). Bottom: $\text{Fe}(\text{OAc})[\text{HB}(\text{3-tBu-5-iPrpz})_3](\text{3-iPr-5-tBupzH})$ (**2**).

solution. These spectral data as well as the results of elemental analysis lead to the conclusion that **2** is the five-coordinate Fe(II) complex with a N_4O_1 ligand donor set consisting of the tris(pyrazolyl)borate, additional pyrazole, and acetate ligands as found in the manganese derivative.²¹ We have reported that various σ -donor ligands such as MeCN and pyridine can bind to the ferrous ion in $\text{Fe}(\text{O}_2\text{CR})[\text{HB}(\text{3,5-iPr}_2\text{pz})_3]$.¹³ A pyrazole can also act as a σ -donor ligand. In addition, the hydrogen-bonding interaction between the pyrazole's NH and the oxygen atom stabilizes the coordination of the additional pyrazole to the metal centers.²¹⁻⁻²³

(b) Hydroxo Complex 3. The IR spectrum of monomeric hydroxo Fe(II) complex **3**, which was prepared by the treatment of a toluene solution of **1** or **2** with aqueous NaOH, contained the O-H vibration at 3695 cm^{-1} . Single crystals of **3** suitable for X-ray analysis were obtained by cooling a mixture of MeCN/ CH_2Cl_2 solution at $4\text{ }^\circ\text{C}$ under an argon atmosphere. As shown in Figure 2 and Table 2, **3** is a slightly distorted tetrahedral complex coordinated by the N_3O_1 donor set (the Fe-O distance is shorter than the Fe-N distances). The iron, oxygen, and boron atoms and one of the pyrazole rings (containing N21) sit on a crystallographic mirror plane. The Fe-O distance ($1.830(8)\text{ \AA}$) is shorter than those in square pyramidal iron complexes such as the dimeric hydroxo complex $[\text{Fe}(\text{HB}(\text{3,5-iPr}_2\text{pz})_3)]_2(\mu\text{-OH})_2$ ($2.016(9)$ and $2.04(1)\text{ \AA}$).¹⁴ To our knowledge, **3** is the first example of a mononuclear tetrahedral Fe(II) hydroxo complex.

(c) Reaction of Hydroxo Complex 3 with Protic Acids. Metal-bound hydroxide ions in $\{\text{M}(\text{OH})[\text{HB}(\text{3,5-iPr}_2\text{pz})_3]\}_n$ (n

(21) The structure of $\text{Mn}(\text{OAc})[\text{HB}(\text{3-tBu-5-iPrpz})_3](\text{3-iPr-5-tBupzH})$ was determined by X-ray crystallography: Komatsuzaki, H.; Hikichi, S.; Kitajima, N.; Moro-oka, Y. Manuscript in preparation.

(22) Kitajima, N.; Osawa, M.; Tamura, N.; Moro-oka, Y.; Hirano, T.; Hirobe, M.; Nagano, T. *Inorg. Chem.* **1993**, *32*, 1879. The hydrogen-bonding interaction between the pyrazole's NH and the oxygen atom of the acetate ligand was suggested on the basis of the short distance between nitrogen and oxygen as well as the absence of a νNH vibration in the IR spectrum.

(23) A hydrogen-bonding interaction between a pyrazole's NH and a peroxide ligand was also observed: Kitajima, N.; Komatsuzaki, H.; Hikichi, S.; Osawa, M.; Moro-oka, Y. *J. Am. Chem. Soc.* **1994**, *116*, 11596.

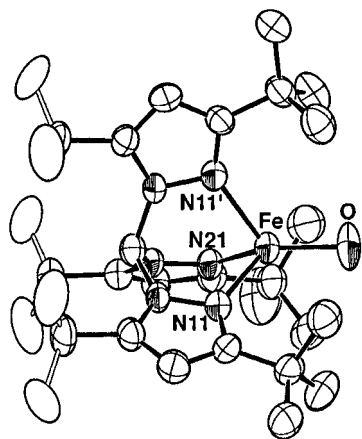


Figure 2. ORTEP drawing of $\text{Fe}(\text{OH})[\text{HB}(3\text{-tBu-5-iPrpz})_3]$ (**3**) (drawn at the 50% probability level). The disordered methyl group carbon atoms at the 5-iPr substituents and all hydrogen atoms are omitted for clarity.

Table 2. Selected Bond Lengths (Å) and Bond Angles (deg) for $\text{Fe}(\text{OH})[\text{HB}(3\text{-tBu-5-iPrpz})_3]$ (**3**)

Bond Lengths					
Fe—O	1.830(8)	Fe—N11	2.103(4)	Fe—N21	2.091(5)
Bond Angles					
O—Fe—N11	123.8(3)	O1—Fe—N21		126.7(5)	
N11—Fe—N11'	92.1(2)	N11—Fe—N21		90.1(1)	

= 1 or 2) are so basic as to react with CO_2 and various protic acids, as we reported previously.^{20c-e,24-27} The monomeric hydroxo $\text{Fe}(\text{II})$ complex **3** also reacted with carboxylic acids to yield the corresponding carboxylato $\text{Fe}(\text{II})$ compounds. The reaction of **3** with benzoylformic acid yielded the monomeric benzoylformato complex $\text{Fe}(\text{O}_2\text{CC}(\text{O})\text{Ph})[\text{HB}(3\text{-tBu-5-iPrpz})_3]$ (**4**). The complex **4** adopted two different structures as confirmed by X-ray crystallography, and the color of the complex could be correlated with the coordination structure as discussed below. On the other hand, the reaction of **3** with benzoylformic acid in the presence of 1 equiv of 3-tBu-5-iPrpzH gave another benzoylformato complex containing an additional pyrazole ligand $\text{Fe}(\text{O}_2\text{CC}(\text{O})\text{Ph})[\text{HB}(3\text{-tBu-5-iPrpz})_3](3\text{-iPr-5-tBupzH})$ (**5**). The molecular structure of **5** was also determined by X-ray crystallography (see below).

Structure and Thermochromism of α -Keto Carboxylato Complexes. (a) **X-ray Crystallography.** X-ray crystallographic studies were performed for two isomers of the pyrazole-free compound **4**, which were crystallized at different temperatures, and the pyrazole-containing complex **5**.

From a MeCN solution of **4** cooled at 4 °C were obtained colorless crystals (colorless form; **4**·MeCN), whereas bluish purple crystals (bluish purple form; **4**· C_5H_{12}) were isolated from a pentane solution of **4** kept at -78 °C for 1 day. The molecular structures and selected bond lengths and angles of the two isomers of **4** are shown in Figure 3 and Table 3, respectively. In the colorless complex, the iron center is coordinated by a tetrahedral N_3O_1 donor set including a unidentate BF (=ben-

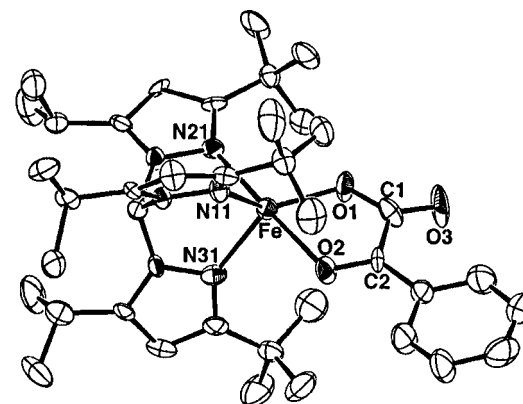
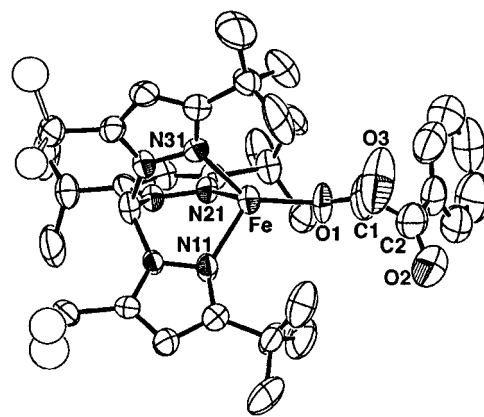


Figure 3. ORTEP drawing of two isomers of a benzoylformato complex (drawn at the 50% probability level). Top: Colorless form of the benzoylformato complex $\text{Fe}(\text{BF})[\text{HB}(3\text{-tBu-5-iPrpz})_3]\cdot\text{MeCN}$ (**4**·MeCN). The disordered methyl group carbon atoms at the 5-iPr substituents, the MeCN molecules of crystallization, and all hydrogen atoms are omitted for clarity. Bottom: Bluish purple form of the benzoylformato complex $\text{Fe}(\text{BF})[\text{HB}(3\text{-tBu-5-iPrpz})_3]\cdot\text{C}_5\text{H}_{12}$ (**4**· C_5H_{12}). The pentane molecules of crystallization and all hydrogen atoms are omitted for clarity.

zoylformate) ligand. The Fe—O1 length (1.889(6) Å) is comparable to the iron—hydroxo bond length of **3** (1.830(8) Å). It is notable that no MeCN molecule is coordinated in the colorless form of **4**, while the MeCN adducts are observed in $\text{Fe}(\text{O}_2\text{CR})[\text{HB}(3,5\text{-iPr}_2\text{pz})_3]$ (R = Ph, Me).¹³ On the other hand, the bluish purple form contains a trigonal bipyramidal iron center where the ketonic oxygen atom (O2) and one of the pyrazolyl nitrogen atoms (N21) occupy the apical positions as judged by the elongated Fe—O2 and Fe—N21 distances (2.261(7) and 2.173(9) Å) and the O2—Fe—N21 angle (177.9(3)°), and the remaining two pyrazolyl ligands and the carboxylate ligand form the basal plane. In contrast to the colorless form, the BF ligand in the bluish purple form works as a chelate ligand through coordination of the carboxylate oxygen atom (O1) as well as the ketonic oxygen atom (O2). The essentially planar chelate ring is arranged coplanar to the phenyl ring. The coordination structure of the BF ligand is close to that found in the six-coordinate benzoylformato complex $[\text{Fe}(\text{O}_2\text{CC}(\text{O})\text{Ph})\cdot(6\text{TLA})]^+$ (6TLA denotes tris[(6-methyl-2-pyridyl)methyl]amine) reported by Chiou and Que.^{16a,b} In the present case, the highly sterically demanding tris(pyrazolyl)borate ligand leads to the tetrahedral and trigonal bipyramidal coordination geometry, while $\text{Fe}(\text{II})$ and $\text{Fe}(\text{III})$ ions favor six-coordinate octahedral geometry.

The structure of the pyrazole-containing benzoylformato complex **5** was also determined as shown in Figure 4. Selected interatomic distances and bond angles are summarized in Table 4. Complex **5** has a distorted trigonal bipyramidal structure

(24) Kitajima, N.; Osawa, M.; Imai, S.; Fujisawa, K.; Moro-oka, Y.; Heerwegh, K.; Reed, C. A.; Boyd, P. D. W. *Inorg. Chem.* **1994**, *33*, 4613.

(25) Hikichi, S.; Tanaka, M.; Moro-oka, Y.; Kitajima, N. *J. Chem. Soc., Chem. Commun.* **1994**, 1737.

(26) (a) Kitajima, N.; Fujisawa, K.; Moro-oka, Y.; Toriumi, K. *J. Am. Chem. Soc.* **1989**, *111*, 8975. (b) Kitajima, N.; Fujisawa, K.; Koda, T.; Hikichi, S.; Moro-oka, Y. *J. Chem. Soc., Chem. Commun.* **1990**, 1357. (c) Kitajima, N.; Fujisawa, K.; Tanaka, M.; Moro-oka, Y. *J. Am. Chem. Soc.* **1992**, *114*, 9232. (d) Kitajima, N.; Katayama, T.; Fujisawa, K.; Iwata, Y.; Moro-oka, Y. *J. Am. Chem. Soc.* **1993**, *115*, 7872.

(27) Hikichi, S.; Tanaka, M.; Moro-oka, Y.; Kitajima, N. *J. Chem. Soc., Chem. Commun.* **1992**, 814.

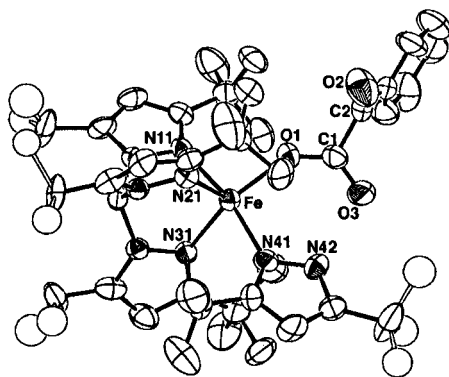


Figure 4. ORTEP drawing of the benzoylformato-pyrazole complex $\text{Fe}(\text{BF})[\text{HB}(3\text{-tBu-5-iPrpz})_3](3\text{-iPr-5-tBupzH})$ (**5**) (drawn at the 50% probability level). The disordered methyl group carbon atoms at the 5-iPr (on the tris(pyrazolyl)borate) and 5-tBu (on the additional pyrazole) substituents and all hydrogen atoms are omitted for clarity.

Table 3. Selected Bond Lengths (Å) and Bond Angles (deg) for $\text{Fe}(\text{BF})[\text{HB}(3\text{-tBu-5-iPrpz})_3]\cdot\text{MeCN}$ (Colorless Form) (**4**·MeCN) and $\text{Fe}(\text{BF})[\text{HB}(3\text{-tBu-5-iPrpz})_3]\cdot\text{C}_5\text{H}_{12}$ (Bluish Purple Form) (**4**· C_5H_{12})

$\text{Fe}(\text{BF})[\text{HB}(3\text{-tBu-5-iPrpz})_3]\cdot\text{MeCN}$ (Colorless Form) (4 ·MeCN)					
Bond Lengths					
Fe–O1	1.889(6)	Fe–N11	2.086(8)	Fe–N21	2.077(6)
Fe–N31	2.087(8)	O1–C1	1.21(1)	O2–C2	1.26(2)
O3–C1	1.19(1)	C1–C2	1.52(2)	C2–C3	1.47(2)
Bond Angles					
O1–Fe–N11	119.7(3)	O1–Fe–N21	115.4(3)		
O1–Fe–N31	135.0(3)	N11–Fe–N21	91.9(3)		
N11–Fe–N31	93.3(3)	N21–Fe–N31	91.1(3)		
Fe–O1–C1	147.8(9)	O1–C1–O3	130(1)		
O1–C1–C2	114(1)	O3–C1–C2	116(1)		
O2–C2–C1	120(1)	O2–C2–C3	118(1)		
C1–C2–C3	122(1)				
$\text{Fe}(\text{BF})[\text{HB}(3\text{-tBu-5-iPrpz})_3]\cdot\text{C}_5\text{H}_{12}$ (Bluish Purple Form) (4 · C_5H_{12})					
Bond Lengths					
Fe–O1	1.975(7)	Fe–O2	2.261(7)	Fe–N11	2.116(9)
Fe–N21	2.173(9)	Fe–N31	2.112(9)	O1–C1	1.27(1)
O2–C2	1.24(1)	O3–C1	1.22(1)	C1–C2	1.59(1)
C2–C3	1.46(1)				
Bond Angles					
O1–Fe–O2	74.3(3)	O1–Fe–N11	129.8(3)		
O1–Fe–N21	103.9(3)	O1–Fe–N31	131.0(4)		
O2–Fe–N11	94.0(3)	O2–Fe–N21	177.9(3)		
O2–Fe–N31	93.9(3)	N11–Fe–N21	88.0(3)		
N11–Fe–N31	97.8(3)	N21–Fe–N31	86.7(3)		
Fe–O1–C1	125.4(7)	Fe–O2–C2	113.8(7)		
O1–C1–O3	129(1)	O1–C1–C2	111(1)		
O3–C1–C2	120(1)	O2–C2–C1	115(1)		
O2–C2–C3	121(1)	C1–C2–C3	124(1)		

with N11 and N41 serving as apical ligands. Because of the steric bulkiness of the *tert*-butyl groups at the 3-position in the tris(pyrazolyl)borate ligand, the pyrazole is bound to the iron as the 3-iPr-5-tBupzH form, as found in the pyrazole-containing acetato Mn derivative. The short N42–O3 distance of 2.70(1) Å suggests a hydrogen-bonding interaction between the pyrazole's NH proton and a carboxylate oxygen atom, which is also supported by the absence of a significant νNH absorption in the range 3300–3100 cm^{-1} .²¹ Such hydrogen bonding probably makes the formation of the 5-coordinated pyrazole adduct possible, while the MeCN adduct has never been observed. Another carboxylate oxygen atom serves as an equatorial ligand; however, the Fe–O_{carboxylate} distance (2.003(8) Å) is somewhat longer than the Fe–O_{basal} of the bluish purple form of **4** (1.975(7) Å). The decrease of the negativity on the carboxylate group

Table 4. Selected Interatomic Distances (Å) and Bond Angles (deg) for $\text{Fe}(\text{BF})[\text{HB}(3\text{-tBu-5-iPrpz})_3](3\text{-iPr-5-tBupzH})$ (**5**)

Interatomic Distances					
Fe–O1	2.003(8)	Fe–N11	2.271(9)	Fe–N21	2.117(9)
Fe–N31	2.102(8)	Fe–N41	2.22(1)	O1–C1	1.26(1)
O2–C2	1.20(1)	O3–C1	1.22(1)	C1–C2	1.53(2)
C2–C3	1.48(2)	N42–O3	2.70(1)		
Bond Angles					
O1–Fe–N11	95.1(3)	O1–Fe–N21	106.8(3)		
O1–Fe–N31	148.4(3)	O1–Fe–N41	95.7(3)		
N11–Fe–N21	85.8(3)	N11–Fe–N31	80.3(3)		
N11–Fe–N41	168.2(3)	N21–Fe–N31	104.0(4)		
N21–Fe–N41	95.5(3)	N31–Fe–N41	88.0(3)		
Fe–O1–C1	142.7(8)	O1–C1–O3	127(1)		
O1–C1–C2	117(1)	O3–C1–C2	116(1)		
O2–C2–C1	120(1)	O2–C2–C3	123(1)		
C1–C2–C3	117(1)				

Table 5. Comparison of Benzoylformato Complexes

complex	4 ·MeCN (colorless)	4 · C_5H_{12} (bluish purple)	5
coord no. of iron atom	4 (distorted tetrahedron)	5 (trigonal bipyramid)	5 (trigonal bipyramid)
coordination mode of BF ligand	unidentate	bidentate	unidentate hydrogen bonding between pyrazole NH and O3)
Bond Lengths (Å)			
Fe–O1	1.889(6)	1.975(7)	2.003(8)
Fe–O2		2.261(7)	
O1–C1	1.21(1)	1.27(1)	1.26(1)
O2–C2	1.26(2)	1.24(1)	1.20(1)
O3–C1	1.19(1)	1.22(1)	1.22(1)
C1–C2	1.52(2)	1.59(1)	1.53(2)
complex	$[\text{Fe}(\text{6TLA})\text{-}(\text{BF})]^+{}^a$	$[\text{Fe}(\text{TPA})\text{-}(\text{BF})\text{(MeOH)}]^+{}^a$	$[\text{Fe}(\text{TPA})\text{-}(\text{BF})(\text{NO})]^+{}^b$
coord no. of iron atom	6 (octahedron)	6 (octahedron)	6 (octahedron)
coordination mode of BF ligand	bidentate	unidentate	unidentate
Bond Lengths (Å)			
Fe–O1	2.001(4)	2.014(6)	2.05(1); 2.05(1)
Fe–O2	2.212(4)		
O1–C1	1.281(7)	1.27(1)	1.23(2); 1.26(2)
O2–C2	1.234(7)	1.20(1)	1.21(3); 1.24(3)
O3–C1	1.211(7)	1.22(1)	1.23(3); 1.22(3)
C1–C2	1.541(9)	1.53(1)	1.51(3); 1.55(3)

arising from the hydrogen-bonding interaction might contribute to the elongation of the Fe–O_{carboxylate} distance.

The coordination environment around the iron ions and the bond lengths of the α -keto carboxylate groups in **4** (two isomers), **5**, and Chiou and Que's complexes are summarized in Table 5. Both the bluish purple form of **4** and the pyrazole-containing complex **5** have pentacoordinated $\text{Fe}(\text{II})$ centers with similar slightly distorted trigonal bipyramidal geometries, although the coordination modes of the BF ligands are different. The coordinated ketonic O2–C2 bond in the bluish purple form of **4** is slightly longer than the noncoordinated O2–C2 bond in **5** (unidentate BF). The elongation of the ketonic bond owing to the chelation of the BF ligand has been also observed in the six-coordinate octahedral $\text{Fe}(\text{II})$ BF complexes reported by Chiou and Que.^{16a,b} On the other hand, the $\text{Fe}(\text{II})$ ion in the colorless form of **4** has a four-coordinate tetrahedral environment and is clearly distinguished from the environment of the iron atoms in the bluish purple form of **4** and **5**. It is notable that the noncoordinated ketonic O2–C2 in the colorless form of **4** (unidentate BF) is the most elongated in the ketonic O2–C2 in the present benzoylformato complexes. In addition, the dis-

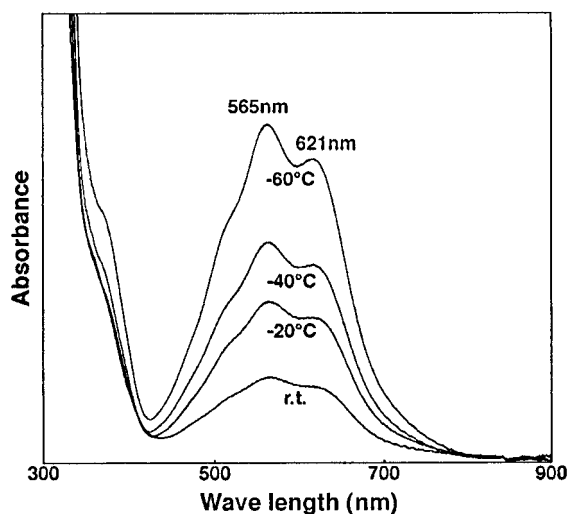


Figure 5. Variable temperature UV-vis spectra of benzoylformato complex **4** in CH_2Cl_2 (1.59 mM).

tances of the Fe-carboxylate moiety (Fe-O1, O1-C1, O3-C1, and C1-C2) in the colorless form of **4** are the shortest in those of the present compounds. In the comparison between two different BF binding mode complexes having the same Fe(II) geometry, such as **5** vs bluish purple form of **4** (trigonal bipyramidal Fe) and/or $[\text{Fe}(\text{TPA})(\text{BF})(\text{MeOH})]$ vs $[\text{Fe}(\text{6TLA})(\text{BF})]$ (octahedral Fe), the noncoordinated ketonic C=O bond is shorter than the coordinated one. Therefore, the unusual observations in the colorless form of **4** can be explained by extensive localization of the electron density on the α -keto carboxylate (i.e., the electron density on the ketonic O2-C2 bond is withdrawn into the carboxylate group), owing to high Lewis acidity of the tetrahedral iron ion.

(b) Solution Behavior. The benzoylformato complex **4** exhibits thermochromism in solution; a CH_2Cl_2 solution of **4** is colorless or pale pink at room temperature, while the color changed to intense bluish purple at lower temperature as characterized by the UV-vis spectra (Figure 5). The color change is correlated with the coordination geometry of the iron center as discussed above. Que *et al.* reported a series of bidentate BF compounds which exhibited intense absorption bands around 500–650 nm, while the unidentate BF compounds had no bands in that region. They assigned the visible bands in bidentate BF compounds as Fe(II) to BF charge transfer (MLCT) bands on the basis of the shift of the λ_{max} values to lower energies with the more electron withdrawing substituents on the phenyl ring.^{16a}

In order to characterize the thermochromism behavior of **4**, variable temperature $^1\text{H-NMR}$ experiments were also performed. The phenyl proton region of the BF ligand is shown in Figure 6. The signal of the *p*-proton is observed at higher magnetic field than the *m*-protons at 27 °C. With cooling to lower temperature (–40 °C), the signal of the *p*-proton shifts to lower magnetic field than the *m*-protons, resulting in the reversal of the chemical shifts of the *p*- and the *m*-protons (Figure 6). This observation suggests that the electron density on the phenyl ring is influenced by the coordination mode of the BF ligand. The coplanar configuration of the BF ligand found in the X-ray study of the bluish purple form corresponding to the lower temperature state suggests π conjugation between the phenyl ring and the α -keto carboxylate group. The shift pattern of the aromatic proton signals observed in this study is consistent with those observed in other benzoylformato complexes previously reported in the literature (unidentate BF, $o < m < p$; bidentate BF, $o < p < m$).^{16a,b} From our experimental results, we conclude that

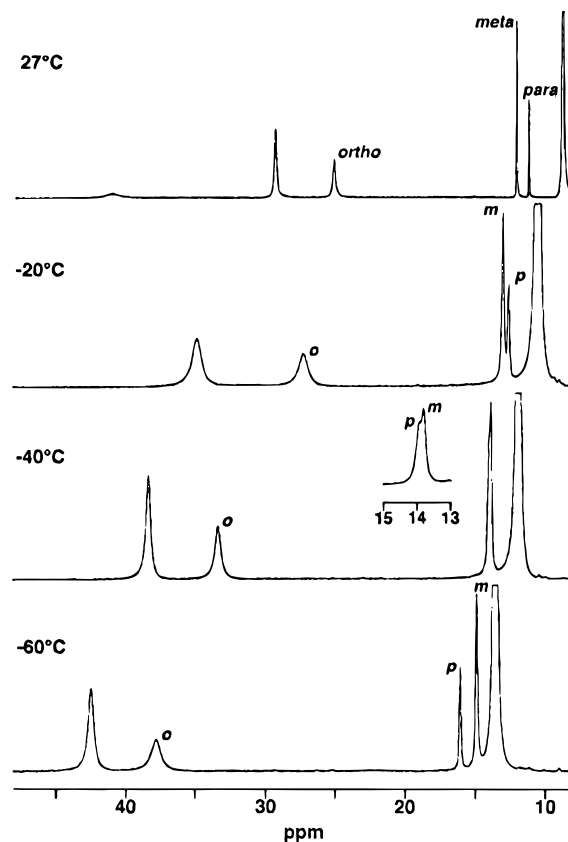


Figure 6. Variable temperature $^1\text{H-NMR}$ spectra (phenyl proton region) of benzoylformato complex **4** in $\text{toluene-}d_8$.

the visible bands in **4** are assigned as Fe(II) to ligand charge transfer bands resulting from the formation of π -conjugated system in the coplanar benzoylformato moiety, as suggested by Chiou and Que.^{16a}

The pyrazole-containing BF complex **5** also shows a thermochromic property similar to that observed for **4**. However, the features of the variable-temperature $^1\text{H-NMR}$ spectra of **5** (data not shown) similar to those of the pyrazole-containing acetate complex **2** suggest the presence of a dissociation equilibrium of the pyrazole ligand. Because of two thermal equilibrium factors (the change of the coordination mode of the BF ligand and the dissociation of the pyrazole), the solution behavior of **5** is complicated.

(c) Reactivity toward Dioxygen. Que *et al.*¹⁶ and Valentine *et al.*¹⁷ recently reported a series of studies of Fe(II) benzoylformato complexes as functional models for α -keto acid-dependent enzymes. Que *et al.* have synthesized the mononuclear $[\text{LFe}(\text{O}_2\text{CC}(\text{O})\text{Ph})]^+$ ($\text{L} = \text{tris}[(6\text{-methyl-2-pyridyl)methyl]amine, 6TLA, and tris}(2\text{-pyridylmethyl)amine, TPA}$)^{16a,b} and dinuclear $[\text{L}_2\text{Fe}_2(\mu\text{-O}_2\text{CC}(\text{O})\text{Ph})]^+$ ($\text{L} = 2\text{-}[(\text{bis}(2\text{-pyridylmethyl)amino)]phenolate, \text{Me}_2\text{HDP}$)^{16c} benzoylformato complexes by using the tetradentate (N_4 or N_3O_1) tripodal ligands. These Fe(II) benzoylformato compounds reacted with dioxygen to induce the oxygenation of the substrates as well as oxidative decarboxylation of α -keto carboxylate to benzoate. Nitrosyl adducts $[\text{LFe}(\text{O}_2\text{CC}(\text{O})\text{Ph})(\text{NO})]^+$ ($\text{L} = 6\text{TLA and TPA}$) have been recently prepared as structural models for the dioxygen adduct of mononuclear active sites of the enzymes.^{16d} Valentine's model compound in particular is closely related to our previous and present work. Valentine and co-workers have adopted the less hindered $\text{HB}(3,5\text{-Me}_2\text{pz})_3$ and obtained the corresponding Fe(II) benzoylformato complex. When the solution of this benzoylformato complex was exposed to O_2 , the solution color changed from blue-purple to green. This

complex is also capable of oxidizing olefinic substrates to give the corresponding epoxide products. On the basis of these results, Valentine *et al.* suggested the formation of a hexacoordinated iron–dioxygen adduct.¹⁷

We have previously reported that a series of monomeric ferrous carboxylato complexes $\text{Fe}(\text{O}_2\text{CR})[\text{HB}(3,5\text{-iPr}_2\text{pz})_3]$ ($\text{R} = \text{Ph}$ and Me) are capable of reacting with dioxygen to form dimeric $\text{Fe}(\text{III}) \mu$ -peroxo species.^{13,15} Other types of monomeric metal complexes such as cobalt²⁸ and copper²⁹ carrying sterically hindered tris(*tert*-butylpyrazolyl)borate ligands such as $\text{HB}(3\text{-tBu-5-Mepz})_3$ and $\text{HB}(3\text{-tBu-5-iPrpz})_3$ are also known to react with dioxygen but give the corresponding monomeric dioxygen adducts. Therefore, the monomeric $\text{Fe}(\text{II})$ complexes synthesized in the present study could be expected to react with dioxygen to yield monomeric iron–dioxygen adducts under appropriate conditions. However, we could not observe the formation of any dioxygen adduct with the benzoylformate and the acetate complexes under various conditions, suggesting that the sterically demanding ligand $\text{HB}(3\text{-tBu-5-iPrpz})_3$ used in this study dramatically reduced the reactivity of $\text{Fe}(\text{II})$ ions toward dioxygen. These results are consistent with our recent observations that monomeric pentacoordinated $\text{Fe}(\text{II})$ complexes having sterically hindered carboxylate ligands, $\text{Fe}(\text{O}_2\text{CtBu})[\text{HB}(3,5\text{-iPr}_2\text{pz})_3]$ and $\text{Fe}(\text{O}_2\text{CAd})[\text{HB}(3,5\text{-iPr}_2\text{pz})_3]$ (O_2CAd denotes 1-adamantylcarboxylate), have failed to form dioxygen adducts probably due to steric congestion around the $\text{Fe}(\text{II})$ ions.^{13b} As shown by X-ray crystallography, the $\text{Fe}(\text{II})$ ions in the present carboxylato complexes are surrounded by the bulky *tert*-butyl substituents. Thus, the $\text{HB}(3\text{-tBu-5-iPrpz})_3$ ligand makes formation of a hexacoordinate $\text{Fe}(\text{III})$ species impossible.³⁰ Our results suggested that, in order to build a suitable (both structural and functional) model for oxygenase enzymes, the ligands that are appropriately designed to retain the reactivity of the metal ions toward dioxygen should be incorporated in the complex.

Structural Comparison with the Monomeric Non-Heme $\text{Fe}(\text{II})$ Centers. The highly sterically demanding $\text{HB}(3\text{-tBu-5-iPrpz})_3$ ligand makes the formation of the monomeric tetrahedral and trigonal bipyramidal $\text{Fe}(\text{II})$ complexes possible, and the structures of the hydroxo complex and the benzoylformate complexes have been determined by X-ray crystallography. We believe that the presented monomeric $\text{Fe}(\text{II})$ complexes may give structural insight into the mononuclear non-heme $\text{Fe}(\text{II})$ site of the several enzymes,^{7–11} although the structures of the α -keto acid-dependent enzymes have not been established.

The structures of the $\text{Fe}(\text{II})$ centers of the enzymes and the synthetic compounds prepared in this work are summarized in Figure 7. In the biological system, a tetracoordinated $\text{Fe}(\text{II})$ ion center containing a unidentate binding carboxylate ligand has been found in soybean lipoxygenase-I (reported by Amzel *et al.*).^{9a} The iron atom is coordinated by the N_3O_1 ligand donor set consisting of three histidyl nitrogen atoms and the unidentate carboxylate oxygen atom originating from the COOH terminus

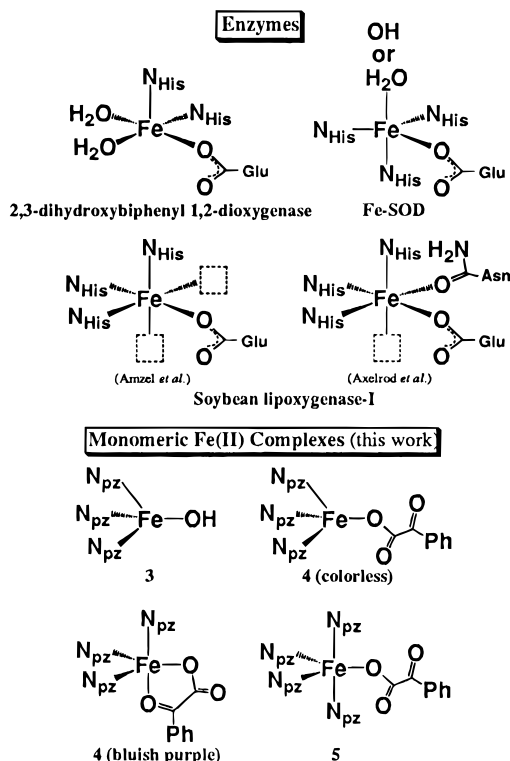


Figure 7. The mononuclear non-heme $\text{Fe}(\text{II})$ centers of the enzymes and the crystallographically characterized complexes in this work.

of the peptide chain (isoleucine residue). However, the geometry around the iron center of the lipoxygenase-I is best described as a highly distorted octahedron with two adjacent unoccupied positions rather than a tetrahedron, and it is clearly distinguishable from those of **3** and the colorless form of **4**. In fact, the $\text{Fe}-\text{O}$ distance in the lipoxygenase (2.07 Å) is longer than those in **3** (1.830(8) Å) and the colorless form of **4** (1.889–(6) Å), although the coordination numbers of the iron atoms are the same. A trigonal bipyramidal iron ion is found in the $\text{Fe}(\text{II})$ center of iron SOD. The trigonal basal plane is composed of the two nitrogen atoms of histidines and the unidentately binding carboxylate oxygen atom of aspartic acid. Apical sites are occupied by the histidyl nitrogen atom and the oxygen atom (OH^- or H_2O) ligands. The $\text{Fe}-\text{N}_{\text{apical}}$ distance (2.18 Å) is slightly longer than $\text{Fe}-\text{N}_{\text{basal}}$ (2.04 and 2.12 Å). The $\text{Fe}-\text{O}_{\text{apical}}$ distance (2.04 Å) is also distinct from the $\text{Fe}-\text{O}_{\text{basal}}$ (1.94 Å).^{7d} The same tendency of the bond lengths (i.e., $\text{Fe}-\text{N}_{\text{basal}} < \text{Fe}-\text{N}_{\text{apical}}$, and $\text{Fe}-\text{O}_{\text{basal}} < \text{Fe}-\text{O}_{\text{apical}}$) is observed in the bluish purple form of **4**, which has similar geometry around the Fe center. Another penta-coordinated $\text{Fe}(\text{II})$ center with a N_2O_3 ligand donor set consisting of two histidyl nitrogen atoms, two water molecules, and a unidentate carboxylate oxygen (glutamate) has been observed in 2,3-dihydroxybiphenyl 1,2-dioxygenase. The geometry of the $\text{Fe}(\text{II})$ ion is best described as a slightly distorted square pyramid, and the carboxylic oxygen atom serves as an equatorial ligand.^{10a}

Summary and Concluding Remarks

By using a novel hindered tris(pyrazolyl)borate ligand, $\text{HB}(3\text{-tBu-5-iPrpz})_3$, a series of monomeric ferrous complexes including acetate, hydroxide, and benzoylformate ligands have been synthesized as structural models for the active sites of the mononuclear non-heme iron enzymes.

The structures of the hydroxo and benzoylformate complexes have been determined by X-ray crystallography. In the case of the benzoylformate complexes, three different coordination

(28) Egan, J. W.; Haggerty, B. S.; Rheingold, A. L.; Sendlinger, S. C.; Theopold, K. H. *J. Am. Chem. Soc.* **1992**, *112*, 2445.

(29) Fujisawa, K.; Tanaka, M.; Moro-oka, Y.; Kitajima, N. *J. Am. Chem. Soc.* **1994**, *116*, 12079.

(30) The tetrahedral $\text{Fe}(\text{II})$ complex **4** (colorless form) yields neither the dioxygen adduct nor the MeCN adduct, although it gives the pyrazole adduct **5**, which is strongly stabilized by the hydrogen-bonding interaction between the carboxylate oxygen atom and the pyrazole NH. In contrast, the dioxygen adduct detectable complexes such as $\text{Fe}(\text{O}_2\text{CR})[\text{HB}(3,5\text{-iPr}_2\text{pz})_3]$ ($\text{R} = \text{Ph}$ and Me)¹³ and $\text{Fe}(\text{BF})[\text{HB}(3,5\text{-Me}_2\text{pz})_3]$ ¹⁷ give the corresponding 6-coordinate MeCN adducts, and the dioxygen adducts are suggested to have 6-coordinate $\text{Fe}(\text{III})$ centers. Therefore, we speculate that the steric demand becomes a dominant factor for reactivity toward dioxygen. However, we have not performed yet a theoretical study about the possibility of formation of a 5-coordinate $\text{Fe}(\text{III})$ -superoxo species.

structures of the benzoylformate ligand are observed. The interatomic distances between the iron atoms and the hydroxyl and the carboxyl oxygen atoms might be influenced by the coordination geometry of the Fe(II) ions.

The benzoylformate complex exhibits thermochromism which depends on the coordination mode of the benzoylformate ligand. Variable-temperature $^1\text{H-NMR}$ experiments reveal clearly that the change of the electronic density on the benzoylformate moiety is caused by the change of the coordination structure of the benzoylformate ligand attached to the iron center. On the basis of structural and spectroscopic studies, the bluish purple color in the chelated benzoylformate complex is considered to be due to metal to ligand charge transfer arising from the π electron conjugation between phenyl and α -keto carboxylic groups due to the planar configuration of the benzoylformate moiety.

The highly sterically demanding $\text{HB}(3\text{-tBu-5-iPrpz})_3$ ligand makes the formation of the tetrahedral and trigonal bipyramidal

Fe(II) complexes possible, while the reactivity of the Fe(II) center toward dioxygen is reduced.

Acknowledgment. We thank Prof. H. Suga (SUNY at Buffalo) for kind help in manuscript preparation and stimulating discussions. This work was supported in part by a Grant-in-Aid for Scientific Research from the Ministry of Education, Science, Sports and Culture, Japan. S.H. was supported by the Research Fellowships of the Japan Society for the Promotion of Science for Young Scientists.

Supporting Information Available: Tables S-1–S-5, containing a summary of the X-ray analysis, isotropic and anisotropic thermal parameters, and interatomic distances and bond angles, and Figures S-1-1–S-1-4, containing ORTEP diagrams including all non-hydrogen atom labels, for **3**, **4**·MeCN (colorless form), **4**·C₅H₁₂ (bluish purple form), and **5** (28 pages). Ordering information is given on any current masthead page.

IC960903M